# Wind turbine wake measurement in complex terrain

**KS Hansen[1,2], GC Larsen[1], R Menke[1], N Vasiljevic[1], N Angelou[1], J Feng[1], WJ Zhu[1], A Vignaroli[1], W Liu W[3], C Xu[4] and WZ Shen[1]**

[1] Department of Wind Energy, Technical University of Denmark
[2] Nils Koppels Allé, B403-DTU, DK-2800 Kgs. Lyngby, Denmark,
[3] North West Survey and Design Institute Hydro China Consultant Corporation (NWI), Xi'an, China
[4] Hohai University, Nanjing, China

E-mail: kuhan@dtu.dk

**Abstract**. SCADA data from a wind farm and high frequency time series measurements obtained with remote scanning systems have been analysed with focus on identification of wind turbine wake properties in complex terrain. The analysis indicates that within the flow regime characterized by medium to large downstream distances (more than 5 diameters) from the wake generating turbine, the wake changes according to local atmospheric conditions e.g. vertical wind speed. In very complex terrain the wake effects are often "overruled" by distortion effects due to the terrain complexity or topology.

## 1. Introduction

Flow in complex terrain displays different characteristics compared to flow over flat and homogeneous terrain. This is due to local distortion effects, which affects both the flow field and the local turbulence. Because the local distortion effects are highly site dependent, complex terrain flow is somewhat more difficult to predict than flow over flat terrain [1]. Installing wind turbines in complex terrain increases the degree of complexity further due to wake effects, and the power production is difficult to correlate to single point wind speed measurements. More research is needed to improve the existing wind farm prediction models for use in complex terrain, and such improvements require validation through field measurements.

Turbines in a wind farm, located in complex terrain are distributed in irregular patterns with different hub heights. The current research will focus on identifying the wake loss between pairs of wind turbines in a wind farm located in complex terrain, furthermore, the wake analysis will be supported by a wake analysis based on detailed wind speed measurements recorded with WindScanners mounted on a hilly site around a single large wind turbine at another location.

The current research project focuses on:

- a characterization of the flow through the wind farm; and
- a wake deficit analysis, which will quantify the maximum wake deficit, the width of the lateral deficit distribution and the behavior of the wake deficit in the flow regime extending from small to medium downstream distances from the wake generating turbine from near to the medium wake area.

## 2. Measurements and data qualification

### *2.1. Presentation of the field locations*

The wind farm consists of 25 x 2 MW wind turbines and are located in a complex terrain in the northern part of China. The 25 wind turbines are erected within an area of 3 x 5 km in an irregular grid as shown in Figure 1. The internal turbine spacing in the wind farm varies between 4 and 10 rotor diameters (D). The inflow from east and south are dominated by a significant terrain complexity, while the inflow from north is dominated by a small and constant terrain slope, Figure 2.

The second field location includes a single wind turbine located on a ridge in Portugal. This site is dominated by two large parallel NW-SE oriented ridges with a separation of approximately 1100 m,

Content from this work may be used under the terms of the Creative Commons Attribution 3.0 licence. Any further distribution of this work must maintain attribution to the author(s) and the title of the work, journal citation and DOI.
Published under licence by IOP Publishing Ltd

Figure 4. The specification of both wind turbines types are listed in Table 1, and they seems to be rather equal concerning size and control.

### *2.2. Description of the measurement setup*

The measurement setup for the two sites are quite different. The focus for the wind farm analysis is on the distributed power production combined with a detailed analysis of the flow around one of the turbines with a "challenging" location on the edge of an escarpment. The focus for the second setup is to quantify the wake behaviour around the investigated wind turbine for various atmospheric situations.

### *2.3. Wind farm in complex terrain*

A large program for measuring flow characteristics in complex terrain has been initiated as part of the Danish/Chinese FarmOpt research program. This project will focus on SCADA measurements from 25 individual wind turbines from a wind farm located in complex terrain, combined with wind speed, turbulence and atmospheric stability measurements from two 70 m masts located close to wind turbine wt#14. One mast and wind turbine wt#14 are located next to the escarpment, while the second mast is located on the escarpment, Figure 1. The smallest turbine spacing (4 – 8 diameters) occurs for westerly and easterly inflow sectors. A contour plot of the surrounding 9.6 x 9.6 km landscape, which illustrates the large complexity for easterly inflow directions, is shown in Figure 2.

The wind climate, cf. Figure 3, has been measured prior the wind farm installation and shows two prevailing wind directions, which should enable a wake study near wind turbine wt#14.

### *2.4. Single wind turbine in complex terrain*

The field measurement program [2] includes many tasks, but of interest for this research is measurement of flow field around a single wind turbine on a mountain ridge. The most interesting flow directions for studying wake characteristics is perpendicular to the ridge as illustrated in Figure 4. The resulting dataset includes wind turbine SCADA data as well as short-range (SR) and long-range (LR) WindScanner measurements. Unfortunately, the wind turbine wake measurements performed with either SR or LR systems do not overlap – in time.

The SR system consist of three synchronous operated LiDAR's, which measures a vertical flow field continuously during 600 seconds at a fixed position NE to the turbine. During southwesterly winds, the LiDAR setup measures the wind turbine wake.

The LR system consists of three long-range synchronous WindScanners. The diamond scanning mode is performed 2 x 10 minutes per hour and represents a horizontal plane (slightly inclined with 4°) around the turbine hub height as shown in Figure 4.

### *2.5. Qualification of SCADA data and mast measurements*

The qualification of the SCADA data [5] included a filtering process to identify periods with icing, periods with wind turbine events (start or stop), idling or curtailment. Such periods are marked properly but not eliminated. Similar icing problems have also been identified for the mast measurements.

An equivalent rotor wind speed is defined as the uniform wind speed that would result in the same power production as the real sheared flow - for each wind turbine. This wind speed is derived from the measured power and pitch values in combination with the official power curve. The equivalent rotor wind speed from a group of "undisturbed" wind turbines are used to quantify the sector-wise inflow wind speed to the wind farm. Currently the wind direction measured on mast M1 is used to characterize the inflow wind direction for the whole wind farm.

### *2.6. Qualification of remote sensing measurements*

Qualification of the measurements has included an internal synchronisation between SR, LR WindScanner measurements and the wind turbine SCADA data. Afterwards, all periods and scanning modes has been identified, indexed and visualised in plots with reference to the SCADA data. Despite

the short campaign period, luckily a limited number of wake periods with inflow perpendicular to the ridge has been identified.

## 3. Analysis

The analysis is divided into two parts:

- Single wind turbine flow measurements;
- SCADA data analysis from the wind farm.

### *3.1. Analysis of the wake conditions recorded with remote sensing for a single wind turbine.*

Most of the data qualification and the analysis have been presented in [4], and furthermore there is a huge amount of plots (>10.000), which are available on request. Results from the diamond scans, presented in Figure 5, demonstrate how the wake deficit at hub height extends more than 3D behind the rotor. In this example there is no visible speed up effect at the ridge.

For this inflow direction the wake deficit can be extracted 1D, 2D and 3D behind the rotor with reference to the averaged wind speed next to the rotor plane. Figure 6 shows a typical lateral wake deficit distribution (as defined in [5]) equal to $(1-U_{wake}/U_{free})$ behind the rotor. The wake expansion increases downstream, compared to the initial rotor diameter of 82 m. SR measurements can provide corresponding horizontal distributions 1D downstream as shown in Figure 7 and Figure 8. The magnitude of the wake deficit (peak value) and the shape of the deficit distribution are almost similar to the results obtained from the diamond scans despite different scanning time and different inflow conditions. The measured wake deficit distribution 1D behind the rotor with the SR WindScanner is shown in Figure 7, here the wake center is moved slightly below the rotor center. Figure 9 shows a similar distribution, but here the wake center clearly is lifted up above the rotor center. These two wake distributions are labelled “DOWN” and “UP” respectively. The LR WindScanner wake measurements in Figure 5 demonstrates a long wake deficit extension while the LR WindScanner wake measurement in Figure 10 demonstrates a very short wake deficit extension. These two wakes are labelled “LONG” or “SHORT” respectively.

### *3.2. Discussion of wake deficit findings*

All the wake vertical deficit distributions and visible wake deficit extension have been categorized according to the above categories: SR-DOWN, SR-UP, LR-LONG, LR-SHORT and visualized together with both horizontal and vertical wind speeds in Figure 11.

Based on the recordings in this figure it can be seen that:

- LR measurements with a short (LR-short) wake occurs during daytime (6:00-21:00);
- LR measurements with a long (LR-long) wake occurs during evening and nighttime;
- SR measurements with lifted wake deficit center (SR-up) occurs during daytime or early evening;
- SR measurements with wake deficit center moved down (SR-down) occurs during nighttime (20:00-01:00), furthermore;
- The measured and averaged SR vertical wind speed is positive during daytime and negative during nighttime.

These findings are indicating a diurnal dependency of the wake propagation. Unfortunately, the vertical wind speed has only been measured with the SR system. A categorization for this system could not be carried out for all available periods due to an unclearly defined wake shape or incomplete scans.

### *3.3. Analysis of wind farm SCADA data from complex terrain.*

The inflow conditions (characterized by wind speed and wind direction at hub height) have been defined in section 2.5. Due to the limited amount of available SCADA data, the best representation for the whole 360 degrees inflow occurs for a wind sped bin of [3;5m/s]. Individual, normalized and averaged wind turbine power values has been extracted for a wind speed bin of 4±1 m/s and 10 degree sectors, and the resulting individual power polar is shown in Figure 12. The figure illustrates the power

variability across the wind farm for all inflow directions [0;360°] representing the wind speed range [3;5m/s]. The figure furthermore includes the average park power production ($\mu_{PN}$) and standard deviation ($\sigma_{PN}$). The biggest terrain complexity occurs for easterly winds and results in a very large power variability (more than ±100%), compared to the average power. Inflow from the western sector results in a much more uniform wind farm production, and the figure demonstrates a smaller variability of ±15%, which also is reflected in the standard deviation.

The most frequent wake situations occurs in the western wind sector where, according to the wind farm layout displayed in Figure 1, the turbine interspacing ranges between 4D and 8D. The wake deficit between pairs of wind turbines has been identified and listed in Table 2. The wake deficit for the "opposite" direction is difficult to identify, due to high terrain complexity and large directional variability combined with low sector occurrence. Furthermore, the measured wind direction from mast M1/M3 is uncertain outside the 210-260° sector.

A visualization of deficit distributions (fitted) for different spacing are shown in Figure 13. The two most distinct distributions occurs between turbines wt#8/wt#10 and wt#5/wt#7 based on the combined high deficit peak value and narrow distributions (<20 degrees). For 5D, 6D and 7D spacing, most of the distributions tend to be averaged over a larger sector with a lower peak values in the range of 30%. A zoom to the westerly inflow sector of the power polar, Figure 14, does not reveal a distinct visual identification of wake effects. The peak indication (~271°) for wt#7 in Figure 14, is expected to occur near 281° based on geographical coordinates and this illustrates the uncertainty of the wind direction.

### *3.4. Discussion of wake analysis*

The large variability in the power signals for easterly wind does not include wake deficits but primarily terrain effects, while the smaller variability in the power for westerly inflow includes some wake effects. A detailed flow analysis of the wake deficit near wt#14 as function of turbulence and atmospheric stability characteristics requires more data, and the result should be compared with the single wind turbine WindScanner results.

## 4. Conclusion

The single wind turbine wake analysis indicates that the wake center moves either upwards or downwards depending on the atmospheric conditions. Especially during daytime we have noticed an upward moving wake center, which seems to correlate with the measured vertical wind speed. During nighttime the wake moves downwards and seems to follow the mountain, but this cannot be confirmed from the present measurements. The LR WindScanner results indicate that the beyond 3D, the wake seems to dilute quickly due to the recirculation on the lee side of the mountain and this happens in a zone poorly covered by the LR WindScanner.

Preliminary results from the analysis of the SCADA data indicates that a major part of the potential wake deficit distributions for spacing in the range 4 – 8 D can be identified. Inflow sectors with moderate complexity seems to demonstrate wake effects, while the wake effect seems to be eliminated completely for sectors with a high complexity.

## 5. Future work

This paper presents some preliminary results based on 6 months SCADA data recorded during wintertime. More data, recorded during summertime, will enable a robust classification of the atmospheric stability from the 3D sonic time series.

- The single wake measurement lacks information about the atmospheric stability and a more systematic registration of the vertical wind speed at hub height.

- The obtained wake deficit distributions from the single wake measurements need to be classified to determine wake expansion as function of different parameters e.g. wind speed, turbulence, yaw misalignment and atmospheric stratification.
- A calibration of the inflow wind direction in the wind farm is required and could be based on grouping the "undisturbed" wind turbine yaw positions in the future. Challenges: the wind turbine yaw positions are not calibrated.
- Model validation based on a large dataset with a representative number of measurements for all inflow directions and a large range of wind speeds.

## 6. Acknowledgement

Farmopt was funded by the Energy Technology Development and Demonstration Program in 2013 (EUDP), UniTTe was supported by The Danish Council for Strategic Research (DSF) in 2013 and New European Wind Atlas (NEWA), which is supported by the EUROPEAN COMMISSION.

## 7. References

[1] Lange, J. et al. For wind turbines in complex terrain, the devil is in the detail, under review in Nature Energy, 2016.
[2] Vasiljević N., Experimental investigation of flow over a double ridge with several Doppler lidar systems presented by at 96th American Meteorological Society Annual Meeting, January 2016, New Orleans, LA.
[3] WAKEBENCH Best Practice Guidelines for Wind Farm Flow Models. 1st Edition IEA Task 31 Report to the IEA-Wind Executive Committee April 2015.
[4] Menke R. Investigation of wind turbine wake propagation in complex terrain, based on WindScanner measurements from the Perdigão experiment, DTU Wind Energy E-0123 report, May 2016.
[5] Hansen KS, Barthelmie RJ, Jensen L, Sommer A. The impact of turbulence intensity and atmospheric stability on power deficits due to wind turbine wakes at Horns Rev wind farm. Wind Energy 2012; 15(1): 183–196. DOI: 10.1002/we.512.

*Table 1: Wind turbine specifications*

| | Wind turbine 25 x Model 1 | Wind turbine 1 x Model 2 |
|---|---|---|
| Name | CSIC H93-2.0MW | E-82 |
| Dia-meter | 93 m | 82 m |
| Power | 2.0 MW | 2.0 MW |
| Hub height | 67 | 78 m |
| Power control | Variable speed & Single blade pitch control | Gearless variable speed, single blade pitch control |

*Table 2: Wake peak deficit between pairs in westerly wind.*

| spacingD | wt1# | wt2# | WD deg | Peak % | Width deg | Slope |
|---|---|---|---|---|---|---|
| 4 | 8 | 10 | 260 | 47.8 | 20 | -4% |
| 4 | 18 | 3 | 273 | 22.7 | 16 | 8% |
| 5 | 14 | 22 | 277 | 43.5 | 24 | -3% |
| 5 | 11 | 13 | 269 | 41.1 | 27 | -3% |
| 5 | 12 | 15 | 253 | 34.7 | 24 | -6% |
| 5 | 4 | 6 | 260 | 29.7 | 30 | 14% |
| 5 | 1 | 2 | 257 | 27.9 | 26 | 8% |
| 5 | 21 | 25 | 260 | 22.6 | 24 | -1% |
| 5 | 14 | 17 | 280 | 16.4 | 16 | -5% |
| 6 | 5 | 7 | 271 | 55.7 | 20 | 11% |
| 6 | 18 | 2 | 170 | 43.4 | 24 | -19% |
| 6 | 3 | 5 | 221 | 33.6 | 20 | 23% |
| 6 | 16 | 21 | 290 | 27.6 | 40 | -11% |
| 6 | 15 | 20 | 277 | 21.9 | 20 | -4% |
| 6 | 2 | 4 | 229 | 19.4 | 25 | 6% |
| 6 | 7 | 8 | 245 | 17.1 | 20 | -2% |
| 6 | 19 | 23 | 250 | 13.7 | 16 | -3% |
| 6 | 20 | 24 | 245 | 4.7 | 16 | -3% |
| 7 | 16 | 19 | 199 | 40.6 | 20 | 0% |
| 7 | 10 | 9 | 156 | 35.3 | 24 | -2% |
| 7 | 12 | 14 | 329 | 34.6 | 20 | -5% |
| 7 | 2 | 5 | 279 | 34.2 | 24 | 22% |
| 7 | 17 | 20 | 197 | 33.1 | 20 | -2% |

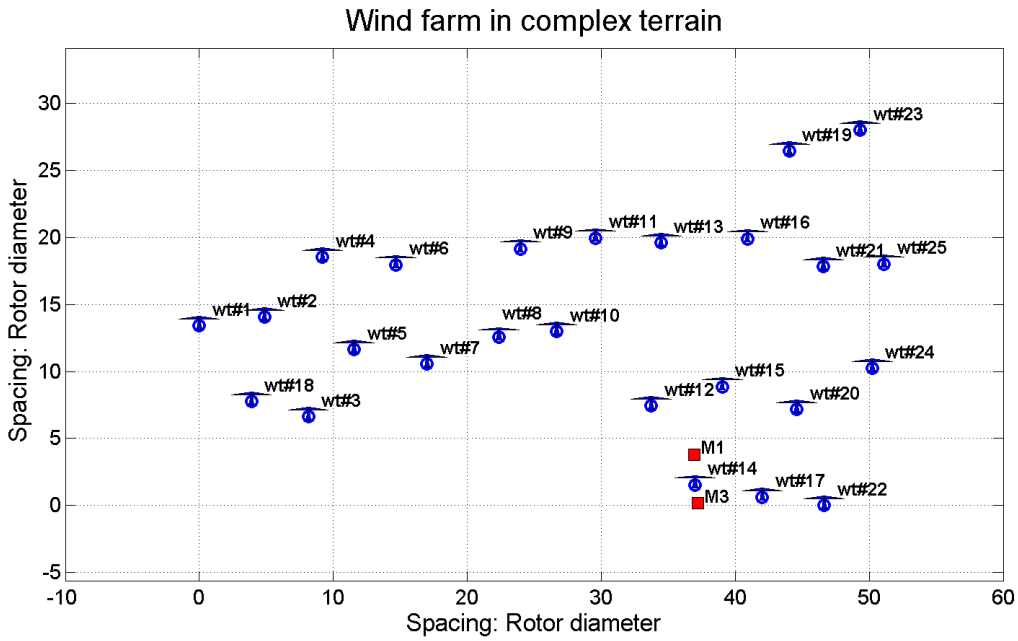



*Figure 1: Layout for a wind farm in complex terrain, the unit is equal to rotor diameter. Two mast are located next to turbine wt#14 - next to an escarpment.*

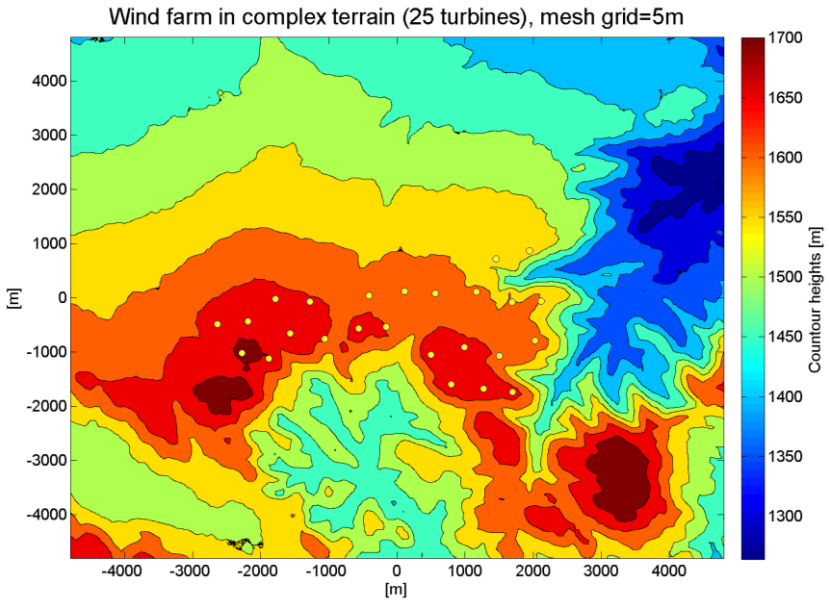



*Figure 2: Wind farm landscape contour plot including location of 25 wind turbines (the white circles represent the wind turbines).*

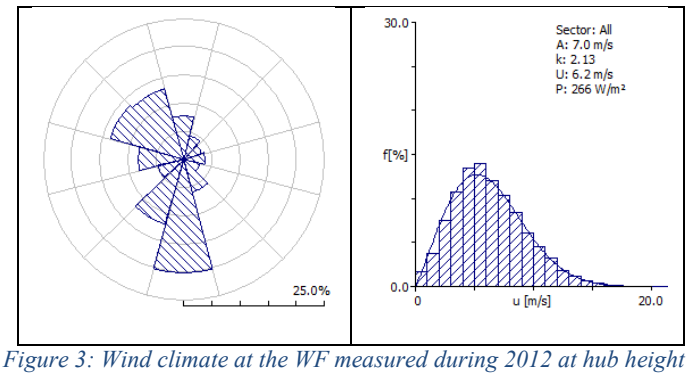



*Figure 3: Wind climate at the WF measured during 2012 at hub height - recorded before the wind turbine installation.*

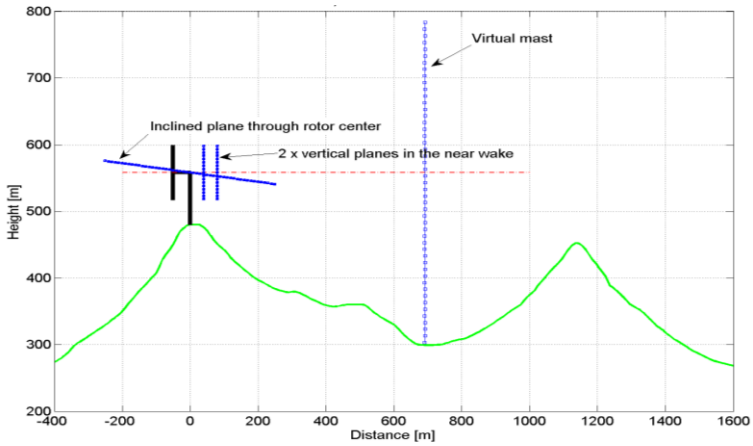



*Figure 4: Measurement setup for the single wake measurement. The dashed 4° inclined dashed line illustrates the diamond long range scanning plane through the hub. The short vertical lines behind the rotor illustrates the short range plane.*

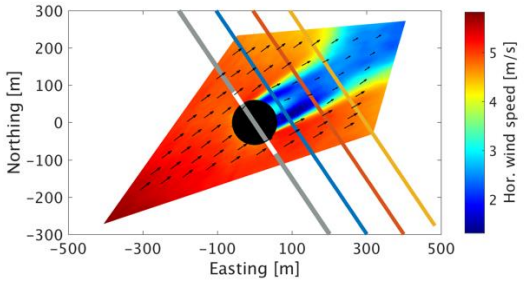



*Figure 5: Horizontal wind speed distribution at hub height around a wind turbine, located on a NW-SE oriented ridge with a LONG wake sector.*

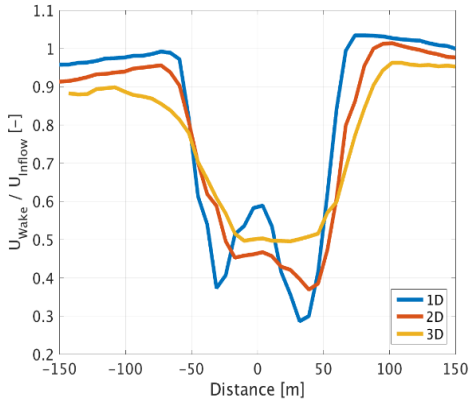



*Figure 6: The horizontal wind speed profiles across the wake sector demonstrates a speed reduction at hub height - 1D, 2D & 3D downstream.*

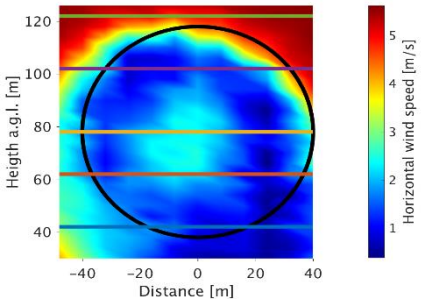



*Figure 7: Horizontal wind speed distribution across the rotor disk – 1D downstream from the rotor disk. The wind speed distribution is recorded with the short-range WindScanner. DOWN*

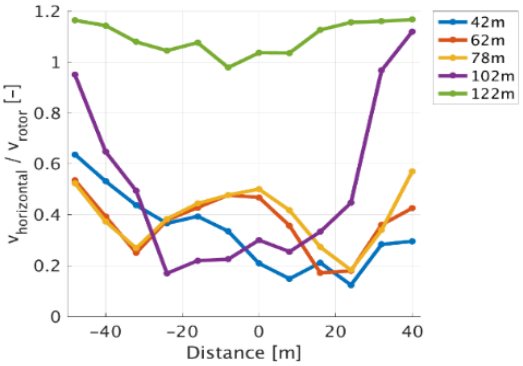



*Figure 8 Horizontal wind speed profiles across the wake at 5 heights including hub height (78 m) - 1D downstream*

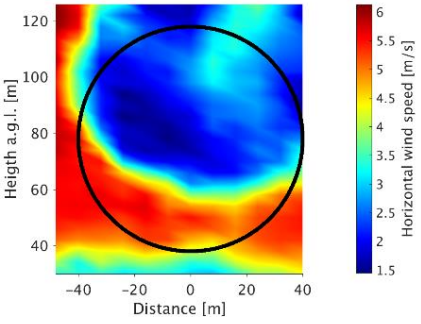



*Figure 9: Horizontal wind speed distribution across the rotor disc, where the wake has been lifted - UP.*

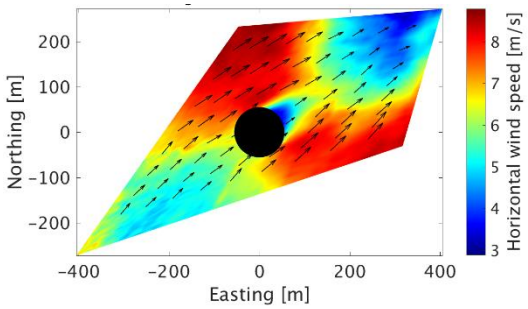



*Figure 10: Horizontal wind speed distribution at hub height around a wind turbine, for a SHORT wake length.*

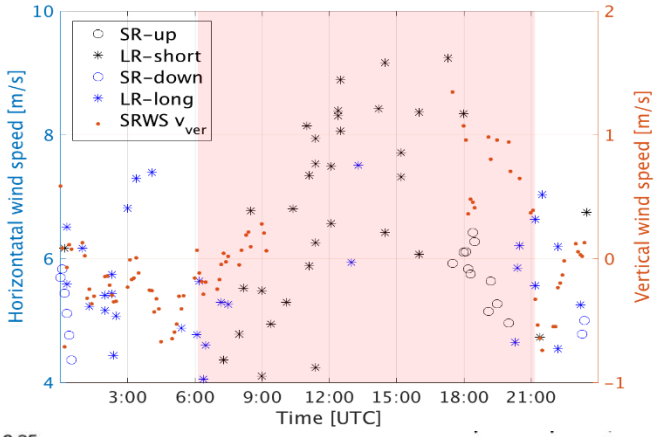



*Figure 11: Diurnal cycle of the vertical wind speed and an indication of the wind turbine wake movement.*

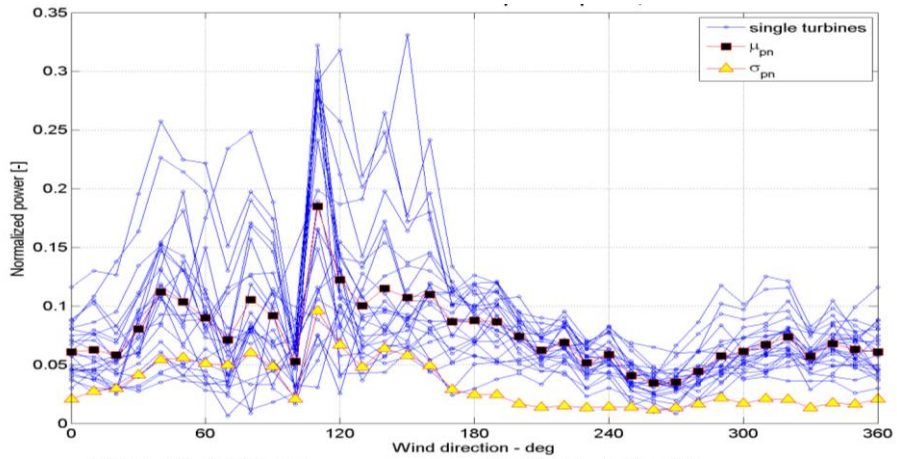



*Figure 12: Normalized sector-wise mean power for each wind turbines. Furthermore, the figure includes the normalized and average park power production ($\mu_{PN}$) and standard deviation ($\sigma_{PN}$).*

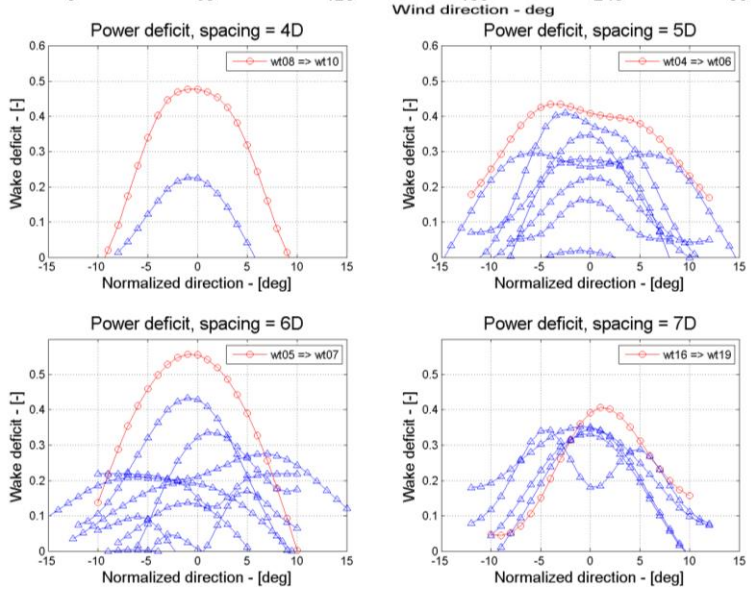



*Figure 13: Power deficit (fitted) distributions between pairs of turbines with 4, 5, 6 or 7D spacing.*

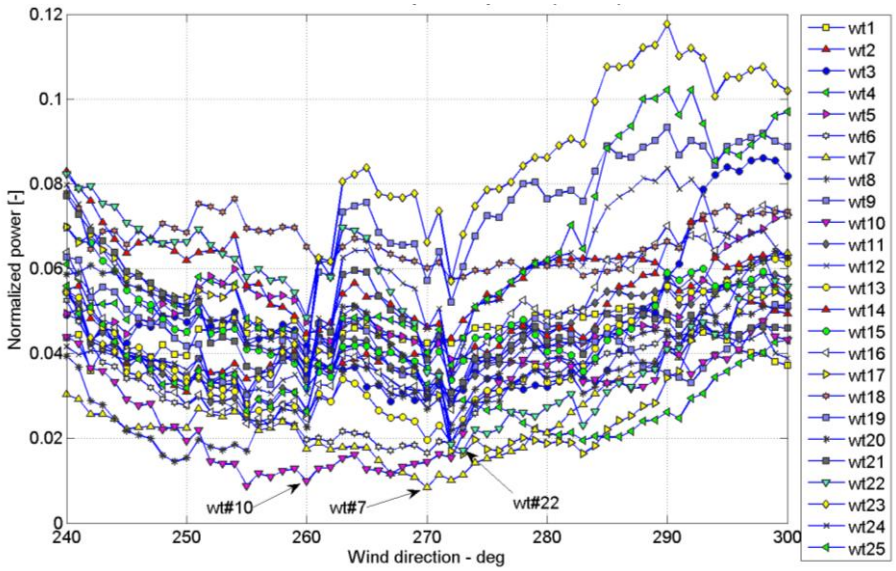



*Figure 14: Zoomed normalized wind turbine power for $U_{hub}$=4±1 m/s*